Effect of radiation-induced mean wavelength shift in optical fibers on the scale factor of interferometric fiber optic gyroscope at a wavelength of 1300 nm*

Jin Jing(金 靖)†, Wang Xue-Qin(王学勤), Lin Song(林 松), and Song Ning-Fang(宋凝芳)

School of Instrument Science and Optic-electronics Engineering, Beijing University of Aeronautics and Astronautics, Beijing 100191, *China*

(Received 25 December 2011; revised manuscript received 6 April 2012)

In order to analyze the effect of wavelength-dependent radiation-induced attenuation (RIA) on the mean transmission wavelength in optical fiber and the scale factor of interferometric fiber optic gyroscopes (IFOGs), three types of polarization-maintaining (PM) fibers is tested by using a ^{60}Co γ-radiation source. The observed different mean wavelength shift (MWS) behaviors for different fibers are interpreted by color-center theory involving dose rate-dependent absorption bands in ultraviolet and visible range and total dose-dependent near infrared absorption bands. To evaluate the mean wavelength variation in fiber coil and the induced scale factor change for space-borne IFOG under low radiation dose in space environment, the influence of dose rate on the mean wavelength is investigated by testing four germanium (Ge) doped fibers and two germanium–phosphorus (Ge–P) codoped fibers irradiated at different dose rates. Experimental results indicate that the Ge-doped fibers show the least mean wavelength shift during irradiation and their mean wavelength of optical signal transmitting in fibers will shift to shorter wavelength in low-dose-rate radiation environment. Finally, the change in the scale factor of IFOG resulting from the mean wavelength shift is estimated and tested, and it is found that the significant radiation-induced scale factor variation must be considered during the design of space-borne IFOG.

Keywords: space radiation, fiber optic gyroscope, scale factor, mean wavelength

PACS: 42.81.–i, 42.88.+h, 42.25.Hz **DOI:** 10.1088/1674-1056/21/9/094220

1. Introduction

Interferometric fiber optic gyroscope (IFOG) is a kind of rotation sensor that can be used to measure position and attitude. As one of the most successful commercial fiber sensors, IFOG has particular advantages for spacial applications, such as good reliability for resting part, very low angular random walk, low mass, low power consumption, and high angular resolution.[1−3] However, space radiation effects on optical components may deteriorate the performance of IFOG. The main contribution to the degradation of IFOG is considered as the radiation-induced attenuation in fiber coil. The radiation-induced attenuation (RIA) in fiber can induce the degradation of IFOG random walk coefficient through decreasing the optical power in the light path and the variation of scale factor because the wavelength-dependent RIA can cause the mean wavelength shift (MWS) when optical signal transmits in optical fiber. The RIA in fibers and its induced degradation in IFOG have been well investigated.[4−7] However, the investigation on radiation-induced MWS and its influence on IFOG's scale factor are surprisingly rare. Friebele *et al.* mentioned that the filtering effect arising from the wavelength-dependent RIA in the fiber coil can cause a change in the scale factor of IFOG, but no experimental results coexist.[8] Boucher *et al.* tested the change of wavelength centroid with time for fiber coil during proton irradiation and showed a steady shift in wavelength.[6] However, as the authors themselves pointed out, the influence of temperature on the light source wavelength shift is not eliminated in this study, which made it ambiguous whether the observed optical wavelength shift resulting from imposed radiation or just from light source drift. In addition, the effect of dose rate on the MWS is not studied, which precludes the prediction of wavelength shift in space environment.

Here, to achieve a definite knowledge of the

*Project supported by the National Natural Science Foundation of China (Grant No. 61007040).

†Corresponding author. E-mail: jinjing@buaa.edu.cn

© 2012 Chinese Physical Society and IOP Publishing Ltd

radiation-induced MWS in polarization-maintaining (PM) fibers and the induced scale factor variation in IFOG, three kinds of PM fibers are tested at 1310 nm using a ^{60}Co γ-radiation source. The characteristics of MWS with respect to the radiation dose after correction by the light source drift are obtained for Ge-doped fibers and Ge–P-codoped fibers. The relationship between the dose rate and the MWS of Ge-doped fibers is also investigated. On this base, the possible variation of IFOG's scale factor in space environment is estimated and tested.

2. Theory and analysis

2.1. Wavelength dependence of fiber's RIA at 1300 nm

The interaction of nuclear radiation with fiber produces defects by trapping electrons and holes at intrinsic precursor sites, and atomic displacements occur via either knock-on or radiolysis process.[9] These defects are termed as color centers. Extensive relevant investigations have been performed in the past decades, and various types of color centers have been identified, including E' centers, non-bridging oxygen hole centers, the peroxy-radical and self-trapped holes.[10] Each color center can absorb light at selective wavelengths, and all color centers give rise to a series of overlapping absorption bands that are strongly wavelength-dependent.[11] Because the light sources used in IFOG are broadband, the wavelength dependence of fiber's RIA can induce the variation of mean wavelength in fiber.

Color centers contributing to fiber's RIA at 1310 nm can be divided into two main terms: (1) the long tail of absorption bands in ultraviolet (UV) and visible range that decreases dramatically with increasing wavelength; (2) the near infrared (NIR)-absorbing band that increases with increasing wavelength. Those NIR-absorbing bands are dependent on total dose, whereas the absorption bands in UV and visible range are dependent mainly on dose rate which have a tendency towards saturation with increasing total dose.[12,13] The competition between these two contributions can govern the MWS of the broadband optical signal transmitting in the fiber coil of IFOG.

The RIA at near-infrared wavelengths is usually assumed to be small as it results from the UV–visible absorption tail, which decreases with increasing wavelength. Therefore, the RIA at 1550 nm is usually considered lower than that at 1310 nm. However, several literatures reported that NIR-absorbing defects play an important role in the fibers' RIA at 1310 and 1550 nm. Therefore, the RIA in optical fibers does not monotonically decrease with increasing wavelength, and the RIA at 1310 nm can be smaller than that at 1550 nm.

2.2. Effect of the mean wavelength on the scale factor of IFOG

The IFOG is a ring interferometer based on Sagnac effect which measures small phase difference between two counter-propagating light paths in a fiber coil produced by the rotation rate:[14]

$$\phi_{\rm s} = G\Omega = \frac{2\pi LD}{\lambda c}\Omega, \tag{1}$$

where L and D are the length and average diameter of the fiber coil, λ is the mean wavelength of light propagating through all optical path, c is the free-space velocity of light, Ω is the rotation rate, and G is the Sagnac scale factor which is defined as the basic sensitivity of the phase shift $\phi_{\rm s}$ to the rotation rate Ω. The scale factor only depends on the ratio LD/λ. The stability of scale factor is therefore directly related to the stability of the mean wavelength in light path.[15] The MWS induced by the wavelength-dependent RIA in fiber during transmission therefore directly dictates the variation of scale factor in IFOG.

The wavelength was measured by an optical spectrum analyzer. The mean wavelength represents the center of mass for all the trace points. The mean wavelength can be calculated by the centroid of the spectrum weighted, which can be approximated by a linear weighting factor

$$\lambda = \frac{\sum\limits_{i=1}^{n} p(\lambda_i)\lambda_i}{\sum\limits_{i=1}^{n} p(\lambda_i)}, \tag{2}$$

where the sample spacing in the spectrum scan is 0.1 nm, and $p(\lambda_i)$ is the optical power at wavelength λ_i.

3. Experimental setup

Three types of fibers with different dopants were chosen in our experiments. Table 1 lists their main characteristics and test parameters. All fibers are Ge-doped core PM fibers with pure silica cladding. Furthermore, there were P-doped ones in Fibers 2 and 3.

For the strict volume and weight requirement of spaceborne IFOG, the cladding and coating diameters of all chosen fibers are 80 and 165 μm, respectively. The operating wavelength of all fibers is 1310 nm. Fibers 1-2, 2, and 3 were respectively employed to compare the difference between different kinds of fibers, and four fibers (1-1, 1-2, 1-3, 1-4) were used to analyze the dose rate effect.

Table 1. Main characteristics and test parameters of fibers.

Fiber	Dopant	Fiber length/km	Cut-off wavelength/nm	Dose rate/Gy·min^{-1}	Total dose/Gy
1-1	Ge	0.129	1148.0	0.0051	42.534
1-2		0.253	1248	0.087	725.58
1-3		0.096	1169.0	0.59	4920.6
1-4		0.073	1201.0	5.2	43368
2	Ge, P	0.147	1106.5	0.087	725.58
3	Ge, P	0.250	1210	0.087	725.58

Test benches shown in Fig. 1 were developed to measure the evolution of MWS in fibers. A superluminescent diode (SLD) with a mean wavelength of 1302 nm and a spectrum width of 43.5 nm was used as the light source, and its output optical signal was split into multiple paths by a splitter. One of them was used as the reference to observe and compensate for the drifts of the SLD mean wavelength, and the others were used as interrogation signals. The interrogation signal power is about 20 μW, which is close to the average optical power transmitting in the fiber coil of one kind of IFOG. Both the mean wavelength of the transmitted optical signal from PM fibers and the reference signal were measured by an optical spectrum analyzer (OSA) in turn. The SLD, light splitter, and OSA were located behind a shielding layer to avoid the influence of radiation on their performance. The mean wavelength of the output optical signals from all fibers was measured before irradiation and at some radiation dose points during the irradiation. Moreover, in order to evaluate the effect of radiation-induced MWS on the scale factor in IFOG, the scale factors of an IFOG with fiber coils winded by the Fibers 1-2 and 3 were tested before and after radiation.

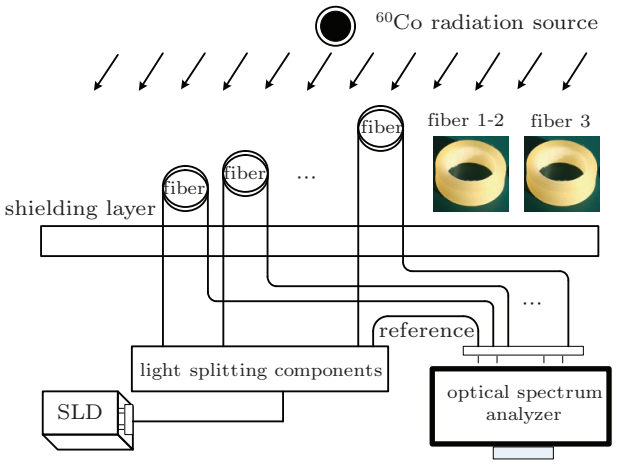


Fig. 1. (colour online) Schematic of experimental setup.

These fibers were irradiated by the ^{60}Co γ-radiation source. The ambient temperature of the irradiation room is 23 °C. The dose rate can be adjusted by increasing or decreasing the distance from the source. The experiment lasted for 139 hours. The radiation dose rate and total dose of fibers are listed in Table 1.

4. Results

4.1. Variation of the mean wavelength in different fibers

The dose-dependent MWS for the three types of fibers and the reference signal of optical source were illustrated in Fig. 2. Different characteristics of MWS were obviously seen. Fibers 2 and 3 show significant decrease in the mean wavelength, but the mean wavelength in Fiber 1-2 slightly increases. The mean wavelength of optical source is relatively stable.

In order to eliminate the influence of the wavelength shift of the light source on the mean wavelength in fiber, the MWS was corrected by the reference signal. Table 2 shows the radiation-induced MWS for the three types of fibers at the same radiation condition after being corrected by the reference signal. The MWS were normalized by using unit nm/km.

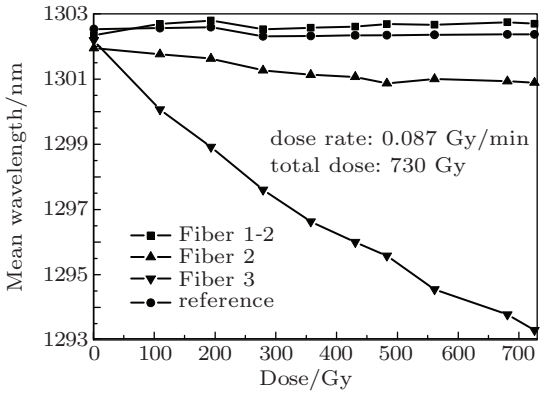


Fig. 2. Dose dependent MWS in three types of fibers and the reference signal.

Table 2. Radiation-induced MWS for the three fibers at the same dose rate of 0.087 Gy/min and total dose of 730 Gy.

Fiber	MWS/nm	Fiber length/km	Normalized MWS/nm·km^{-1}
1-2	0.515	0.253	2.036
2	–0.8936	0.147	–6.079
3	–8.7249	0.250	–34.900

The measured spectra of Fiber 2 during irradiation were shown in the Fig. 3. The noise of spectra increases during irradiation induced by the radiation-induced attenuation in optical fiber. The noise of measured spectra of Fiber 3 increases much remarkably than Fiber 2 because of larger RIA and longer length. The measured spectra of Fiber 1 do not show significant variation of noise characteristics for its much smaller RIA during irradiation. As can be seen from Fig. 3, the RIA in longer wavelength is larger than that in shorter wavelength, which confirms the influence of P1 centers.[11]

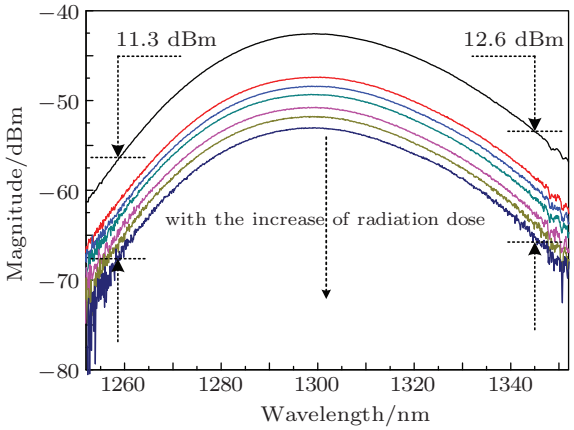


Fig. 3. (colour online) Variation of the output optical spectrum from Fiber 2 during irradiation.

4.2. Influence of the dose rate on the variation of mean wavelength

The radiation-induced MWS at different dose rates for four same-type fibers are illustrated in Fig. 4. The MWS data were corrected by the reference signal. Fibers 1-2, 1-3, and 1-4 exhibit a wavelength shift towards longer wavelength, which is characterized by a sharp mean wavelength increase in the initial exposure period followed by a gentle slop. By contrast, Fiber 1-1 at the lowest radiation dose rate shows a slight decrease of mean wavelength, which is similar to the P-doped fiber. Table 3 gives the normalized MWS for the four fibers which were irradiated at different dose rates.

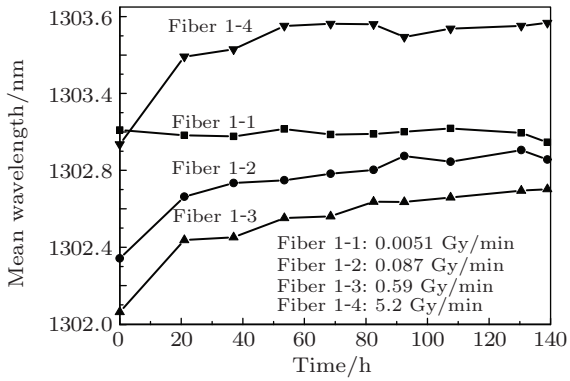


Fig. 4. MWS behaviors of Fiber 1 at different dose rates.

Table 3. Radiation-induced MWS for same-type fibers at different dose rates.

Fiber	Dose rate /Gy·min^{-1}	Fiber length/km	Normalized MWS/nm·km^{-1}
1-1	0.0051	0.129	–0.493
1-2	0.087	0.253	2.036
1-3	0.59	0.096	6.657
1-4	5.2	0.073	8.649

The RIA data of all experimental fibers are plotted in Figs. 5 and 6 to help to analyze the MWS behavior. Fibers 2 and 3 show large RIA up to 112.4 and 47.7 dB/km at a dose of 730 Gy, respectively. The RIA in the fibers at low doping level is smaller than that in the fibers at high doping level. The RIA of fiber at low dose rate is smaller than that at high dose rate. The larger RIA in Fibers 2 and 3 should be ascribed to the influence of P1 center with large RIA.[16] The radiation-induced attenuation A obeys a power law of radiation dose:

$$A = gd^f, \tag{3}$$

where g and f are constants, and d is the radiation dose. The fitting results of the three fibers at the same dose rate of 0.087 Gy/min and total dose of 730 Gy by Eq. (3) and radiation dose are listed in Table 4.

Table 4. Fitting results of RIA model.

Fiber	g	f
1-2	0.1201	0.558
2	0.2855	0.7823
3	1.143	0.7029

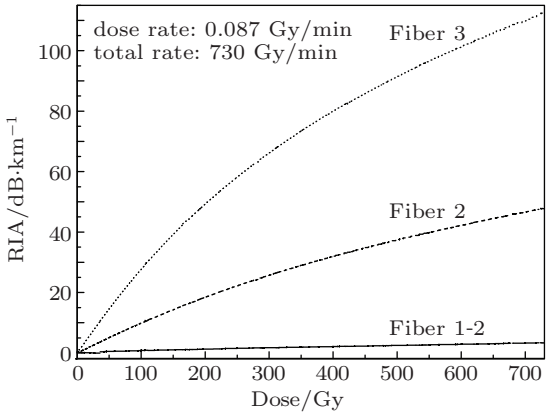


Fig. 5. RIA of three different types of fiber at a dose rate of 0.087 Gy/min and total dose of 730 Gy.

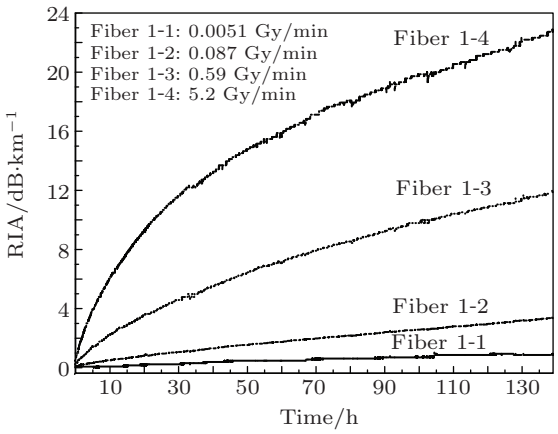


Fig. 6. RIA of Fiber 1 at four different dose rates.

5. Discussion

5.1. MWS for different kinds of fibers

For steady irradiation, the P1 defects with an absorption peak at around 1600 nm are the main origin of RIA in Ge–P-codoped fibers at NIR waveband, and it contributes more than 80% to the total RIA at 1310 nm.[11] Obviously, within the optical spectrum range of our SLD optical source, light attenuation caused by P1 defects will increase with increasing wavelength. Hence the mean wavelength in Ge–P-codoped fibers will shift toward blue during irradiation, resembling Fibers 2 and 3 illustrated in Fig. 2. The different slopes of wavelength change in Fibers 2 and 3 are assumed to be related to the different doping level. Moreover, like other NIR color centers, the amount of P1 defects increases with increasing radiation dose. Therefore, the blue shift of the mean wavelength at 1310 nm keeps increasing with the radiation dose without apparent plateau at lease in the experimental radiation dose region.

For Ge-doped fibers without phosphorous doping, previous studies have confirmed that there is also a total dose-dependent NIR-absorbing band.[13,17] Although the nature of this absorbing band is still not clear, it is known that its absorption at 1310 nm is much weaker than absorption from P1 color center, and also usually weaker than the long tail of absorption bands in UV and visible range.[11] Thus, the long tail of UV and visible absorption bands is the dominant contribution to the RIA at 1310-nm waveband in Ge-doped fibers, so the mean wavelength shifts to red after irradiation, resembling Fiber 1-2 illustrated in Fig. 2. Moreover, given the dose-rate-dependent nature of absorption bands in UV and visible range, the resulting RIA will gradually saturate with continuous radiation when the generation and decay of color centers reach equilibrium. Thus, the MWS-radiation time profile of Fiber 1-2 (see Figs. 2 and 4) exhibits a sharper increase in the mean wavelength in the beginning exposure period followed by a gentle slop, which differs from the Ge–P-codoped fibers.

5.2. MWS for same-kind fibers at different dose rates

Given relatively small MWS, the radiation dose rate effect of Ge-doped fibers was studied. As mentioned above, the dominant absorption bands of Ge-doped fibers resulting from UV and visible color centers decrease with reducing dose rate. Hence, the normalized MWS of Fibers 1-2, 1-3, and 1-4 decreases with decreasing dose rate, as shown in Table 3. However, when the radiation dose rate is sufficiently small, influence of the NIR absorption band on the RIA at 1310-nm waveband is dominating instead of the long tail of UV and visible absorption like the Ge–P-codoped fiber. Fiber 1-1 at a much smaller dose

rate of 0.0051 Gy/min confirms this case, in which the mean wavelength shifts to blue. The situation is contrary for Fibers 1-2, 1-3, and 1-4 irradiated at relatively high dose rates.

5.3. Scale factor variation in IFOG induced by MWS

According to Eq. (1), the scale factor is inversely proportional to the mean wavelength. Thus, the MWS during irradiation can cause the variation of scale factor in IFOG that can be computed based on Eq. (1).

Table 5 gives the calculated results and tested results of the scale factor variation in IFOG using Fibers 1-2 and 3 irradiated at a dose rate of 0.087 Gy/min and the total dose up to 725.58 Gy. As can be seen, both the calculated variations and the tested variations of scale factors are coincident, and the scale factor in IFOG using Ge–P-codoped fiber coil (Fiber 3) was considerably increased. The scale factor in the IFOG with Ge-doped fiber coil (Fiber 1-2) shows a relatively small decrease. However, according to Section 5.2, a sufficiently low dose rate will convert MWS from red shift to blue shift, which makes the scale factor rise rather than fall. Therefore, in space environment where only a very low radiation dose rate (~ 0.0004 Gy/min) exists, the scale factor increase is expected for both Ge–P-codoped and Ge-doped fibers. Moreover, owing to the strong absorption of P1 color center in NIR region, scale factor variation in Ge–P-codoped fibers should be larger than that in P-free Ge-doped fibers and are less suitable to be used in the space-borne IFOG. However, for Ge-doped fibers, the scale factor variation is also large in space, because with a much smaller radiation dose rate and an extremely prolonged radiation period in space environment, the scale factor increase of Ge-doped fiber is evaluated to be larger than that of Fiber 1-2, which is not a negligible level. Therefore, the scale factor variation for both Ge-doped fibers and Ge–P-codoped fibers should be noted in the design of IFOG.

Table 5. Calculated and tested variation of scale factor in an IFOG.

Fiber	Fiber length/km	MWS/nm	Calculated variation/ppm	Tested variation/ppm
1-2	0.253	0.515	–395.5	–378.1
3	0.250	–8.7249	6701.1	6519

6. Conclusion

The radiation-induced mean wavelength shifts at 1310-nm waveband in PM fibers with different dopants and its effect on the scale factor of IFOG have been investigated. The radiation-induced variation of mean wavelength in different fibers under certain radiation condition and the influence of different dose rates on the variation of mean wavelength were obtained and interpreted using the color-center theory. The radiation-induced mean wavelength shift of P-free Ge-doped fibers was found to be smaller than that of Ge–P-codoped fibers. The radiation-induced MWS of Ge-doped fibers decreases with decreasing dose rate. When the radiation dose rate is sufficiently small, the mean wavelength of Ge-doped fibers shifts to blue, resembling Ge–P-codoped fibers. Based on the investigation on the radiation-induced mean wavelength shifts in different fibers at different radiation dose rates, the variations of scale factor in IFOG induced by MWS were calculated and tested, and the calculated and tested results are coincident.

The present study convinces us that the non-negligible influence of space radiation on the mean wavelength in different fibers deteriorates the scale factor performance of IFOG. Further studies should be conducted to minimize or compensate the scale factor variation in space-borne IFOG.

References

[1] Dollon M, Cros G, Sevellec A, Antoine P, Muller G, Willemenot E, Urgell A, Hardy G, Loret T, Faussot N, Cottreau Y and Gaiffe T 2002 *Proceeding of the 5th ESA International Conference on Spacecraft Guidance, Navigation and Control Systems* October 22–25, 2002 Frascati, Italy, p. 41

[2] Jin J, Tian H T, Pan X and Song N F 2010 *Chin. Phys.* B **19** 030701

[3] Jin J, Xu H J, Ma D Y, Lin S and Song N F 2012 *Opt. Laser. Eng.* **50** 958

[4] Friebele E J, Gingerich M E, Brambani L A, Harrington C C and Hickey S J 1990 *Proc. SPIE* **1314** 146

[5] Friebele E J and Wasserman L R 2006 *18th International Optical Fiber Sensors Conference* October 23–27, 2006 Cancún, México, ME2

[6] Boucher R H, Woodward W F, Shima T S, Asman D J, Killian K M, Legrand J and Goellner G J 1996 *Opt. Eng.* **35** 955

[7] Jin J, Wang X Q, Song N F and Zhang C X 2010 *Sci. China. Tech. Sci.* **53** 3056

[8] Friebele E J, Askins C G, Miller G A, Peele J R and Wasserman L R 2004 *Proc. SPIE* **5554** 120

[9] Cooke D W, Bennett B L and Farnum E H 1996 *J. Nucl. Mater.* **232** 214

[10] Wijnands T, Kuhnhenn J, Hoeffgen S K and Weinand U 2008 *IEEE Trans. Nucl. Sci.* **55** 2216

[11] Regnier E, Flammer I, Girard S, Gooijer F, Achten F and Kuyt G 2007 *IEEE Trans. Nucl. Sci.* **54** 1115

[12] Morita Y and Kawakami W 1989 *IEEE Trans. Nucl. Sci.* **36** 584

[13] Kyoto M, Chigusa Y, Ooe M, Watanabe M, Matubara T, Yamamoto T and Okamoto S 1989 *J. Nucl. Sci. Technol.* **26** 507

[14] Lefèvre H C 1996 *Proc. SPIE* **2837** 1

[15] Gaiffe T, Simonpiétri P, Morisse J, Cerre N, Taufflieb E and Lefèvre H C 1996 *Proc. SPIE* **2837** 375

[16] Girard S, Keurinck J, Meunier J P, Meunier J P and Boukenter A 2004 *J. Lightwave Technol.* **22** 1915

[17] Henschel H, Köhn O and Schmidt H U 1996 *Proc. SPIE* **2811** 68